[1]Zhongcai Gao
[1]Huiqian Zhang*
[2]Jiangqin Chao
[3]Yurong Li
[4]YongjunLi
[5]Jiale An

Research on Slope Stability Prediction Model Based on Topographic and Geomorphic Features

Abstract: - In order to prevent slope collapse in time, this paper firstly collects topographic and geomorphological features to obtain macro and micro feature data such as slope gradient, slope direction and ground rate. Secondly, a model for predicting slope stability is established based on the obtained topographic and geomorphological data, and the topographic and geomorphological data are input into the model to predict the stability of the slope. Finally, through the prediction of the model, the value of slope stability is obtained, so that the imbalance of the slope can be prevented and the occurrence of accidents can be reduced. The results show that the predicted and actual coefficients of safety are 1.23 and 1.22 respectively at a slope of 8m with a low error. The prediction level of the model is better, the actual stability value and the predicted stability value are almost the same, and when predicting the horizontal displacement, the predicted displacement value and the actual displacement value are both 1.2, which can accurately predict the stability of the side. Compared with other models, the GM-RBF model has a safety state error of 0. The prediction model can reinforce the slope in time, reduce the cost of the project, and protect people's safety.

Keywords: slope collapse; topographic and geomorphic features; slope stability; safety coefficient; prediction model

1. INTRODUCTION

In geological engineering, slope stability is closely related to daily life, and if an accident occurs, it will not only cause casualties and threaten people's life safety, but also affect the surrounding ecological environment. In the geological engineering in today's era, the stability of slope is very important, which directly affects the operation of transportation and the stability of roadbed [1-2]. Slope mainly refers to artificially formed slopes, which is a common geomorphological form, the stability of the slope is related to the progress and quality of the project, which affects the stability of the surrounding environment, and once the imbalance of the slope occurs, it will cause a serious geologic disaster, which will damage people's property and personal safety [3-4]. In order to be able to reduce the probability of slope imbalance, the prediction model of slope stability is established, and the stability of the slope is predicted by means of collecting topographic and geomorphological features, so as to reduce the injury of personnel, protect people's property safety, enable the project to be carried out on schedule, accelerate the speed of the project, reduce the cost of the project, ensure the safety of the project and the economy, and promote the positive development of the slope project, which has a high research value and practical value [5].

[1] Faculty of Land Resources Engineering ,Kunming University of Science and Technology, Kunming 650093, Yunnan, China.*Email：hannibalnn@163.com

[2] School of Geographical Sciences and Tourism, Zhaotong University, Zhaotong 657000, Yunnan, China.

[3] Faculty of Land Resources Engineering ， Kunming University of Science and Technology, Kunming 650093, Yunnan, China.

[4] Faculty of Land Resources Engineering ， Kunming University of Science and Technology, Kunming 650093, Yunnan, China.

[5] Faculty of Civil Engineering and Mechanics ， Kunming University of Science and Technology, Kunming 650500, Yunnan, China.

In this paper, firstly, we collect the characteristics of topography and geomorphology, obtain the relevant characteristics and data of topography and geomorphology, and understand the causes of slope imbalance, which is convenient for the establishment of the subsequent model, and improve the accuracy of the model prediction. Secondly, the prediction model GM-RBF is established based on the obtained topographic features, and the stability of the slope is predicted using the GM-RBF model to reduce casualties and prevent traffic congestion. Finally, the performance of the model is evaluated, and it is proved that the model has good prediction ability, which can evaluate the condition of the slope in real time, and reinforce the slope in time to prevent the slope from becoming unbalanced and having accidents, which will cause casualties and affect the ecological environment and the progress of the project. The prediction model is designed to ensure that the project can be completed on schedule and provide new directions and ideas for the establishment of the project.

2. RELATED WORKS

In establishing the stability prediction model based on topography, Huang, S. et al. improved the original k-nearest neighbor algorithm to reduce the dependence of the model. The robustness of the model is improved, and the slope stability is predicted using the improved k-nearest neighbor algorithm, and the evaluation of the test results can be concluded that the model can meet the demand and complete the detection of slope stability [6]. Markovic Brankovic, J. et al. used a neural network model for predicting the stability and safety of the slope, and based on the experiments, the model predicted a better effect and prevented accidents. The model predicts better, prevents accidents and is able to model slopes. The early warning of slope collapse can assist people in daily use, which is more practical and can prevent the occurrence of failures [7]. Pei, T. et al. used physical or data-driven methods to establish a slope stability prediction model, and used physical methods to study the geotechnical engineering knowledge of soil mechanics to analyze the situation of the slope and to detect whether there is a phenomenon of displacement. According to the experiments, the model has a better prediction effect and reduces the probability of accidents [8]. Meng, J. et al. collected slope-related data and used a neural network model to predict the stability of slopes, and trained the network model through the collected data as a way to improve the prediction accuracy of the model. According to the experiments, the prediction effect of the model is better, and it can remind people to pay attention to the slope in time in order to extract and arrange the protective measures [9]. Xie, H et al. utilized the random forest based algorithm to evaluate the stability and safety of the slope. Based on the data of the slope, the factors affecting the stability of the slope were identified, and the prediction model of the slope was constructed from these influencing factors, focusing on checking the possible factors to prevent anomalies in the slope. According to the experiments, the prediction results of the model are similar to the actual results, and the imbalance of the slope is prevented in time [10]. Liu, L. et al. proposed an optimal path forest algorithm based on k-nearest neighbor to predict the stability of the slope. Firstly, the collection of historical slope data of bad risk is initiated to obtain the corresponding slope characteristics. Secondly, the data set is divided by random division, and the divided data set is trained and tested, and the parameters are adjusted by the effect of the test. Finally, the performance of the model is evaluated by using the relevant test indexes, which proves that the predictability of the model is good and meets the current needs [11]. Zhang, H. et al. designed a prediction method of minimizing the edge distance. Firstly, the model was built by collecting the data related to the edge slope and using machine learning. Secondly, the MDMSE algorithm was used to train the data in machine learning. Finally, the data were integrated to form a stability prediction model of the slope using majority voting method, and based on the experiments, it was concluded that the model could accurately predict the results [12].

3. TOPOGRAPHIC AND GEOMORPHOLOGICAL FEATURES COLLECTION

3.1 Topographic feature acquisition

Before predicting slope stability, it is necessary to collect topographic features to facilitate the subsequent construction of the model. Digital geomorphological modeling is used to collect terrain data and obtain the parameters and features of the terrain. The digital geomorphological model usually needs to use visualization technology to improve the digital effect, and restore the characteristics of the terrain according to the dimensions and simulation, and the common methods include vertical section method, geomorphological halo method and perspective map method. Among them, the geomorphic halo method can show the characteristics of the terrain in a comprehensive way, which adopts the form of contrasting light and darkness, and sets the slope facing the light as bright and the slope backing the light as dark, which can show the changes of the ground's undulation and have a strong sense of three-dimensionality.

3.1.1 Macro factors

From a macroscopic point of view in general, the factors that affect the visual effect of the geomorphic vignette map are as follows:

(1) The azimuth angle of the sun, usually around 0° to 360°, the default solar azimuth is 315°.

(2) The sun's altitude angle, the sun's altitude angle mainly refers to the angle between the ground plane and the refracted light of the light source, the variation is from 0° to 90°, the lower the sun's altitude angle, the darker the rendered map. In addition to this, it is also related to the slope and slope direction factors, with slope varying from 0° to 90° and slope direction from 0 to 360°. Transparent parameters are set in the shaded part of the map, and the digital map model is superimposed to enhance the display of the map [13-14].

The elevation statistics are shown in Table 1, and the elevation is divided into four levels by combining the characteristics of the terrain and landscape. The elevations in the map area are generally taken at low elevations below 1000m, accounting for 98.8% of the overall, with an average elevation of about 540m. The predominantly low mountainous areas show a terrain that is high in the northwest and low in the southeast, and the overall area from north to south is characterized by a heavy valley area, a low mountain wide valley area, and a low mountain dam mountain area. Among them, the wide valley low mountain area from 500m to 700m accounts for 50.34% of the total area, and the area from 700m to 1,000m accounts for 40.23% of the total area, with mountain peaks towering into the forests and a more spectacular topography, with thick rock layers in the center, hillocks and platforms in the south, and gullies and valleys in the north.

Table 1 Elevation statistics

Elevation range	**Number of rasters**	**Area/kms**	**Ratios/ %**	**Elevation range**	**Number of grids**	**Area/km**	**Ratios/ %**
<500	321271	289.1439	9	500-800	2689693	2420.724	75.38
800-1000	515814	464.2326	14.46	1000-1300	41232	37.1088	1.20

3.1.2 Micro-indicators

There are many micro-indicators in topographic features, including slope, slope direction and ground rate, etc., in which slope and slope direction are interconnected, and slope is mainly the angle between the horizontal surface and the ground surface in the area, which includes the percentage of slope and the gradient in two ways. Whereas the angle between the horizontal plane and the slope is the gradient, which is used to indicate the inclined state of the slope, that is, the angle between the Z -axis and the surface unit, the average slope is the range of the degree of ground undulation, and the percentage of slope, which is also referred to as descending slope. The calculation was carried out using the fitted curve surface method, S_x, S_y which represents the slope values in the x and y directions, respectively, and the formula is as follows:

$$S = \tan\sqrt{S_x^2 + S_y^2} \tag{1}$$

The slope statistics are shown in Table 2, which shows that it can be concluded that the proportion of flat slopes, i.e., angles less than 5, in the topographic features is 11.07%, the proportion of gently sloping slopes with an angle between 5 and 15 degrees is about 55.99%, and the proportion of slopes with an angle between 15 and 25 degrees is about 28.95%. The percentage of steep slopes with angles between 25 and 35 degrees is about 3.47%, values below 25 degrees, 96.01%, and areas higher than 25 degrees account for 3.99%. This shows that the overall terrain is gentle, including river valleys and hilltops, and that there is a positive relationship between slope and runoff volume, and between the slope of the side slopes and the degree of soil erosion.

Table 2 Slope statistics

Sub-basin code	Number of grids	Area/kms	Percentage of
<3°	1615101	145.359	4.53%
3°-5°	233357	210.0213	6.54%
5°-8°	498061	448.2549	13.96%
8°-15°	1499686	1349.717	42.03%
15°-25°	1032785	929.5065	28.95%
25°-35°	123787	111.4083	3.47%
35°-77°	18224	16.9416	0.52%

Slope direction, also known as slope inclination, mainly refers to the angle between the due north direction and the normal line, which in the actual landscape represents the lower position of the terrain, and can clearly show the overall trend of the terrain, and the due north direction in the geographic coordinate system is usually 0°. According to the clockwise direction metric, between 0 ° and 360 °, will not have a downhill direction of the flat area is useful -1 indicated. Where S_x and S_y denote the slope values in the x and y directions, respectively, the formula is:

$$A = S_y / S_x \tag{2}$$

The trend of the terrain represents the movement characteristics of the tectonic structure, which is used to analyze the movement structure of the mountain, and the slope direction will have an effect on the sunlight and precipitation, and the ecological vegetation will thus appear to be differentiated, and the distribution of the location is different. The digital map model is used to obtain the raster of the slope direction, and the direction is divided according to the isometric method, the area ratio is more similar, the distribution is more scattered, and the slope direction is usually in the direction of the fault, and there is a gentle trend.

In the macroscopic feature extraction of topographic features, including the degree of roughness of the terrain and the degree of undulation of the terrain, a larger range of geomorphic features is demonstrated. Among them, the surface undulation mainly refers to the undulation state produced when the land is eroded, using $H_{\max}$ and $H_{\min}$ to represent the difference value between the maximum and minimum values of the elevation in the region, then the formula for the calculation of the degree of terrain undulation is as follows:

$$RF_i = H_{\max} - H_{\min} \tag{3}$$

The slope direction statistics are shown in Table 3, and it can be concluded that the darker the color on the map, the more undulating the terrain is, while the lighter the color indicates the less undulating the terrain is. The minimum value is 0, the maximum value is 433m, and the average value is around 177, which unfolds the hierarchy of the undulation of the terrain according to the specification. Since the maximum value is less than 500m, the area of tableland is the largest, accounting for about 61.60%, the area of plains accounts for 20.27%, and the area of small undulating mountains is about 0.11%. According to the statistics, the terrace terrain is more, followed by plains and hills, and the number of small undulating mountain terrain is less, and the areas with higher degree of undulation are associated with fracture tectonics [15-16].

Table 3 Slope Direction Statistics

Slope direction	Number of grids	Area/kms	Percentage (%)
Flat (-1)	1812	1.63	0.05
North (0-22.5)	154868	139.38	4.36
Northeast (23.5-69.5)	463529	417.18	13.05
East (67.5-112.5)	547008	492.31	15.40
Southeast (112.5-157.5)	482272	434.04	13.57
South (157.5-202.5)	401609	361.45	11.30
Southwest (202.5-247.5)	488102	439.29	13.74
West (247.5-292.6)	488768	439.89	13.76
Northwest (292.5-337.5)	380771	342.69	10.72
North (337.5-360)	144272	129.85	4.06

3.2 Characterization of water basin areas

When collecting the topography of a water basin, a digital map model, a flow direction matrix and a cumulative matrix are the basis for the topography of the water basin. Since the topography of the water basin can be noisy, the data collected can be wrong, which leads to the failure of collecting a more complete topography of the water basin. This reduces the accuracy of the collection and even makes it difficult to extract the correct water basin topography. Therefore, it is necessary to fill the water basin, clarify the real depressions on the surface of the terrain, mark the incorrect part of the water basin data on the map, and analyze the area of the water basin to determine the area of the depressions by using the direction of the water flow in order to complete the collection of the topography of the water basin.

The flow accumulation is used to indicate the number of rasters passed by the direction of water flow, and the accumulation of high flow is used to indicate the terrain areas where water flow is concentrated and mark the river channels. If the flow value is zero, the place is a high point, using this way to determine where the ridge is located, using the surface runoff diffusion model to start the calculation of the river network, to get the number and location of the river network, in the digital map model according to the maximum slope drop method to determine the direction of water flow, the cumulative number of rasters in the direction of the flow to start the calculation of the number of rasters, reflecting the number of rasters that the water flow direction flowed through the raster location.

The water flow is generated by the return flow reaching a certain value, larger than the critical number of rasters is the water flow path, from the water flow path to form the river network, the collection of the river network topography needs to set the threshold value of the water area, the larger the threshold value, represents the river network density is small, and vice versa, the river network density is large, the watershed is more. The threshold of confluence is set to 100, 1000, 5000 and 10000, by comparing with the actual topography of the watershed, it can be concluded that when the threshold is 100, the density of the river network is high and the number of channels is more, the threshold is more reasonable when it is 1000, which can accurately reflect the topography and characteristics of the watershed, and the threshold is 10000, the density of the river network is larger, and the number of channels is too sparse, so the threshold set at 1000 is more realistic and can accurately capture the characteristics of the topography of the water basin.

4. CONSTRUCTION OF SLOPE STABILITY PREDICTION MODEL

According to the above process to complete the collection of topographic and geomorphological features, to get the topographic and geomorphological data, used to establish the model for detecting the stability of slopes. Gray system theory is used to construct the slope stability prediction model, and the model GM-RBF is obtained, and the prediction process is shown in Figure 1. In the gray system theory, $GM(1,5)$ is an important component, mainly using the cumulative way to turn the irregular raw data into a more regular generating sequence model, and to predict the data [17-18].

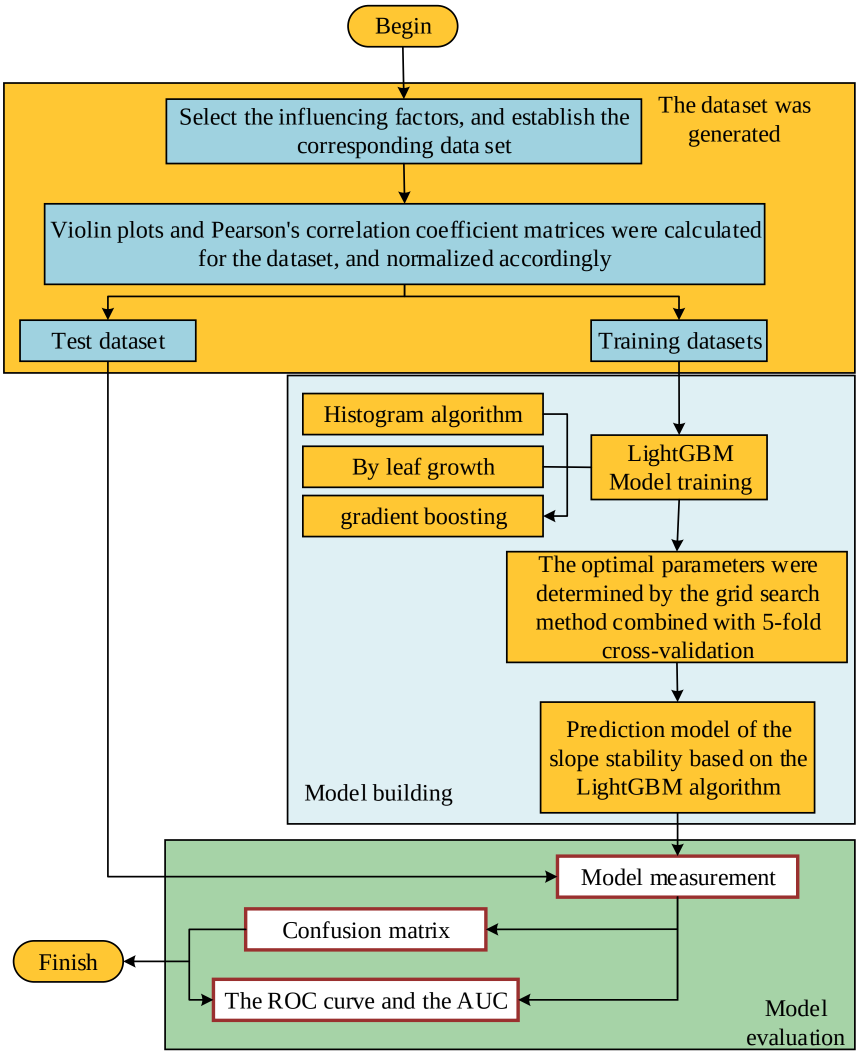

Figure 1 Forecasting process

In the prediction process, cumulative generation is the first and foremost part. Let $x_i^{(0)}(k)$ be a known quantity, the first order accumulation of $x_i^{(0)}(k)$ by cumulative generation generates $x_i^{(1)}(k)$ as follows:

$$x_i^{(1)}(k)=\sum_{j=1}^{k}x_i^{(0)}(j) \tag{4}$$

where $x_i^{(0)}(k)$ represents the original sequence, $x_i^{(1)}(k)$ represents the cumulative sequence, and $i=1,2,3,\cdots,n,k=1,2,3,\cdots,m$.

Let there exists a set of smooth non-negative terrain data consisting of a sequence, using the form of one-time accumulation of the sequence to expand the processing, the generation of a new series in accordance with the exponential form of generating changes, is the basis of the establishment of gray system modeling.

In the gray modeling session, a first order differential equation is established for $x_i^{(1)}(k)$ as follows:

$$\frac{dx_i^{(1)}(k)}{dt}+ax_i^{(1)}(k)=\mu=\sum_{i=2}^{N}b_i x_i^{(1)}(k) \tag{5}$$

Where, μ represents the number of raw ash, a represents the number of developed ash, and b_i represents the parameters.

Using the least squares method to solve the vector expansion of the parameters, the following equation can be obtained:

$$B=\begin{bmatrix} -\frac{1}{2}\left(x_1^{(1)}(1)+x_1^{(1)}(2)\right) & x_2^{(1)}(2) & \cdots & x_N^{(1)}(2) \\ -\frac{1}{2}\left(x_1^{(1)}(2)+x_1^{(1)}(3)\right) & x_2^{(1)}(3) & \cdots & x_N^{(1)}(3) \\ \vdots & \vdots & \vdots & \vdots \\ -\frac{1}{2}\left(x_1^{(1)}(n-1)+x_1^{(1)}(n)\right) & x_2^{(1)}(n) & \cdots & x_N^{(1)}(n) \end{bmatrix} \tag{6}$$

In the above equation, $\hat{a}=\left[a,b_1,b_2,\cdots,b_N\right]^T$ and satisfy condition $\hat{a}=\left(B^TB\right)^{-1}B^TY_N$. Is obtained:

$$Y_N=\left(x_1^{(0)}(2),x_1^{(0)}(3),\cdots,x_1^{(0)}(n)\right)^T \tag{7}$$

The calculation gives the following prediction equation for $GM\left(1,N\right)$:

$$x_1^{(1)}(k+1)=\left[x_1^{(1)}(0)-\frac{1}{a}\sum_{i=2}^{N}b_i x_i^{(1)}(k+1)\right]e^{-ak}+\frac{1}{a}\sum_{i=2}^{N}b_i x_i^{(1)}(k+1) \tag{8}$$

where $x_1^{(1)}(0)=x_1^{(0)}(1)$ unfolds a cumulative operation on the $x_1^{(1)}(k)$ sequence, which reduces the simulated values as follows:

$$x_1^{(0)}(k+1)=x_1^{(1)}(k+1)-x_1^{(1)}(k) \tag{9}$$

The prediction of slope stability requires a combination of scientific and reasonable prediction methods, so on the basis of the $GM\left(1,5\right)$ model, the slope stability is further analyzed using the RBF model [19-20].The

RBF is mainly a neural network structure, which is composed of a nonlinear layer with a kernel function and a linear output layer, and it can use a small number of radial functions to reflect a multidimensional nonlinear system, with a better learning effect and a relatively simple structure with strong approximation ability. It is relatively simple and contains strong approximation ability. In the RBF model, the commonly used function is Gaussian function, as follows:

$$R_i\left(x_p\right)=\exp\left(-\frac{1}{2\sigma_i^2}\| x_p-c_i \|^2\right) \tag{10}$$

where x_p represents the p nd input terrain feature, $x_p=\left(x_1^{(p)}, \quad x_2^{(p)},\cdots x_m^{(p)}\right)^{\mathrm{T}}$ $R_i\left(x_p\right)$ represents the Gaussian function value, with c_i representing the center position in the prediction model, $i=1,2,3,\ldots,m$, $\| x_p-c_i \|^2$ represents the Euclidean paradigm, and σ_i represents the variance.

The output model of the RBF model is shown below:

$$y_i=\sum_{i=1}^{n}\omega_{ij}\exp\left(-\frac{1}{2\sigma_i^2}\| x_p-c_i \|^2\right) \tag{11}$$

where ω_{ij} represents the connection weights, $j=1,2,3,\ldots,m$.

The variance expansion of the Gaussian function can be solved using the clustering algorithm as follows:

$$\sigma_i=\frac{c_{\max}}{\sqrt{2h}} \quad (i=1,2,3,\cdots,h) \tag{12}$$

where h represents the number of feature data at the center of the Gaussian function when training the input features, and $c_{\max}$ represents the maximum value of the center point clustering.

$GM\left(1,5\right)$ and RBF models are obtained through the above process, and the combination of the two can effectively form a predictive model for slope stability.

The univariate and multivariate analysis sequences are established as follows:

$$\begin{gathered}
X_0^{(0)}=\left(X_0^{(0)}(1),X_0^{(0)}(2),\cdots,X_0^{(0)}(n)\right)\\
X_1^{(0)}=\left(X_1^{(0)}(1),X_1^{(0)}(2),\cdots,X_1^{(0)}(n)\right)\\
\vdots\\
X_m^{(0)}=\left(X_m^{(0)}(1),X_m^{(0)}(2),\cdots,X_m^{(0)}(n)\right)
\end{gathered} \tag{13}$$

Due to the differences in the magnitude of the factors between the input terrain feature data, which differ from each other, the accuracy of the prediction needs to be improved. Therefore, the training speed of the network needs to be increased to control the raw terrain data between 0 and 1 and normalized:

$$x_i(k)=\frac{X_i(k)-X_{i\min}}{X_{i\max}-X_{i\min}} \tag{14}$$

Otherwise:

$$\begin{aligned} x_0^{(0)} &= \left(x_0^{(0)}(1), \mathrm{x}_0^{(0)}(2), \cdots, \mathrm{x}_0^{(0)}(n) \right) \\ x_1^{(0)} &= \left(x_1^{(0)}(1), x_1^{(0)}(2), \cdots, x_1^{(0)}(n) \right) \\ &\vdots \\ x_m^{(0)} &= \left(x_m^{(0)}(1), x_m^{(0)}(2), \cdots, x_m^{(0)}(n) \right) \end{aligned} \tag{15}$$

where $X_{i\max}$ and $X_{i\min}$ represent the maximum and minimum values of the sequence, respectively.

The first prediction of the input terrain feature data is carried out using the $GM\left(1,N\right)$ model, and the input terrain feature data are accumulated to produce a parameter sequence value of $\hat{a}$ and a new predicted value sequence value of $\hat{y}^{(1)}$:

$$\begin{cases} d_1 = \hat{y}^{(1)}(k) - x_0^{(0)}(k) \\ d_2 = \hat{y}^{(1)}(k-1) - x_0^{(0)}(k) \end{cases} \tag{16}$$

The RBF neural network model was used to develop the second prediction, and based on the difference between the prediction results obtained from the $GM\left(1,5\right)$ model and the actual values, the difference obtained was taken as the output, and the analyzed sequence of the RBF model was as follows:

$$\begin{aligned} d_1 &= \left(d_1(1), \quad d_1(2), \cdots, d_1(n) \right) \\ d_2 &= \left(d_2(1), \quad d_2(2), \cdots, d_2(n) \right) \\ x_0^{(0)} &= \left(x_0^{(0)}(1), x_0^{(0)}(2), \cdots, x_0^{(0)}(n) \right) \\ x_1^{(0)} &= \left(x_1^{(0)}(1), x_1^{(0)}(2), \cdots, x_1^{(0)}(n) \right) \\ &\vdots \\ x_m^{(0)} &= \left(x_m^{(0)}(1), x_m^{(0)}(2), \cdots, x_m^{(0)}(n) \right) \end{aligned} \tag{17}$$

Consider $x^{(0)}$ as the topographic feature data input to the model, and d_1 and d_2 represent the desired output values as follows:

$$d = \left(d_1, d_2 \right) = \sum_{i=1}^{m} \omega_i R_i(x) = \sum_{i=1}^{m} \omega_i \exp\left(-\frac{\left\| x_p - c_i \right\|^2}{2\sigma_i^{\,2}} \right) \tag{18}$$

where ω_i represents the synaptic weights.

The sequence of training fitted inputs and outputs yields $d_1^{'}$ and $d_2^{'}$ for the predicted outputs, and unfolding the computation on the sequence of differences yields the following equation:

$$\hat{y}^{(0)}(k) = d_1^{'} - d_2^{'} \tag{19}$$

Expanding the inverse normalization on $\hat{y}^{(0)}(k)$ yields the predicted value $y^{(0)}(k)$ of the GM-RBF model as follows:

$$y^{(0)}(k) = \hat{y}^{(0)}(k) \times \left(X_{0\max} - X_{0\min} \right) + X_{0\min} \tag{20}$$

where $X_{0\max}$ and $X_{0\min}$ represent the maximum and minimum values of sequence X_0, respectively.

According to the above process to complete the establishment of the slope stability prediction model, and get the value of the prediction of slope stability, which is convenient for timely reinforcement of the slope area [21].

5. PREDICTIVE ANALYSIS OF SLOPE STABILITY

5.1 Slope safety factor analysis

The prediction of slope safety coefficient is mainly used to measure the important index of slope stability, which can accurately determine whether the slope is stable or not, whether it needs to be reinforced, etc., and can stabilize the slope in time. The more similar the value of the slope safety coefficient is to the value of the actual safety coefficient, the more accurate the model prediction is, and the more quickly measures can be made for the slope. Timely reminding of the collapse of the slope makes it easy for people to extract and arrange protective measures to avoid losses, so the slope safety coefficient is analyzed. The safety coefficient score is shown in Table 4, and the error between the safety coefficient and the actual safety coefficient is at most 0.2, and the safety coefficient is 1.23 and the actual safety coefficient is 1.22 when the slope is 8m, and the prediction model error is low. The established GM-RBF prediction model has a good prediction effect, and the predicted value is similar to the actual value when the prediction of the safety coefficient is unfolded. When the cohesion force is 22kM, the cohesion force of the slope is 0kPa, the internal friction is 40°, the breaking angle is 33°, and the slope height is 8m, the value of the safety coefficient is 1.15, and the actual value of the safety coefficient is 1.13, and the error of the two is less.

Table 4 Factor of safety scores

Gravity/kN/m	Cohesion /kPa	Angle of internal friction/°	Breaking angle/°	Slope height/m	Safety coefficient	Actual safety coefficient
18.5	12	0	30	6	1.43	1.45
22	0	40	33	8	1.15	1.13
20	0	24.5	20	8	1.23	1.22
27	50	40	20	8	1.4	1.42
18	0	30	33	8	1.58	1.60
22	10	35	30	10	0.81	0.83

The GM-RBF model is compared with the GM(1,5) model and the RBF model, and Fig. 2 shows the prediction curves of slope safety coefficients of different models. In the case of the same sample training sequence of 30, the GM-RBF prediction model can accurately predict the slope safety coefficients, and the difference between the actual value and the predicted value is 0.1 at most, so that it reminds people to carry out the slope reinforcement in a timely manner. It can be seen that the predicted value and the actual value of GM-RBF model are almost the same, and the prediction ability is better compared with the other two, mainly because the GM-RBF model combines the GM(1,5) model and the RBF model, extracting the strengths of the two models, so that the prediction ability is stronger, which is in line with the current needs.

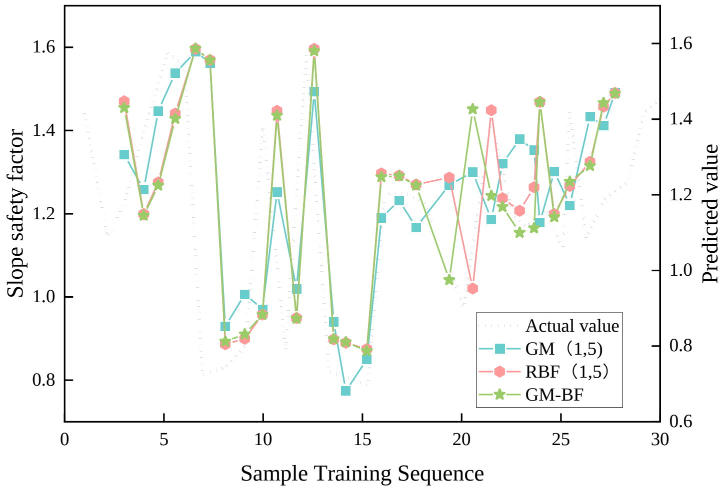

Figure 2 Prediction curves of slope safety coefficients for different models

5.2 Predictive analysis of slope deformation and displacement

Slope deformation and displacement are the main indicators to determine the stability of slopes, once the slope displacement and deformation, the slope will face the risk of collapse, which is easy to cause casualties and traffic congestion, affecting the surrounding environment. Monitoring the deformation and displacement of slopes can help to understand the deformation trend and speed of slopes, assess the stability of slopes in time, and reinforce the slopes to prevent them from collapsing and threatening people's lives. Therefore, it is necessary to analyze the prediction of slope deformation and displacement, and Table 5 shows the analysis of slope deformation and displacement prediction. It can be concluded that the proposed method is more accurate in predicting the deformation and displacement of the slope, which is similar to the actual value, even in the third prediction, the predicted and actual values of horizontal displacement are 1.2, and the predicted and actual values of vertical displacement are -0.5, which is almost the same as the actual value, and the predicted results and the actual value are almost the same, and it can be a better assessment of the degree of stability of the slope. If the deformation and displacement of the slope reaches a certain value, people can be reminded to reinforce the slope in time to reduce the damage to people's property and safety and avoid potential risks.

Table 5 Predictive analysis of slope deformation and displacement

Ordinal number	Horizontal displacement	Actual value	Vertical displacement	Actual value
1	0.5	0.6	-0.2	-0.3
2	0.8	0.9	-0.3	-0.2
3	1.2	1.2	-0.5	-0.5
4	0.3	0.2	0.1	0.2
5	0.5	0.6	-0.3	-0.2

5.3 Predictive analysis of slope stability

Slope stability prediction is mainly used to measure the accuracy of the model prediction, whether it can correctly predict the stability of the slope. That is, whether the results predicted by the model and the actual value are consistent, if the two are similar, it proves that the model can prevent the collapse of the slope in time and reinforce the slope. So the stability prediction of the slope is analyzed, and the comparison of the prediction accuracy of different methods transaction is shown in Table 6.The stability prediction of GM-RBF model is better. The error value is less. By comparing the stability prediction of GM(1,5), RBF and GM-RBF models, it can be concluded that at the actual value of 1.32, the GM(1,5) model predicts 1.204 with an error of 8.79%.The RBF model predicts 1.42 with an error of 7.58%. And the GM-RBF model predicted 1.29 with an error of 2.27%. Compared with the other two approaches, the error is less and the accuracy is higher, indicating that the GM-RBF model can accurately predict the stability of the slope.

Table 6 Comparison of transaction prediction accuracy of different methods

Number of times	Actual value	GM (1, 5) model		RBF model		GM-RBF model	
		Predicted value	Error	Predicted value	Error	Predicted value	Error
1	1.32	1.204	8.79%	1.42	7.58%	1.29	2.27%
2	0.97	1.123	15.77%	0.901	7.11%	0.952	1.86%
3	1.578	1.451	8.05%	1.495	5.26%	1.523	3.49%
4	0.88	0.746	15.23%	1.025	16.48%	0.964	9.55%
5	1.58	1.214	23.16%	1.311	17.03%	1.526	3.42%
6	1.412	1.594	12.17%	1.325	6.76%	1.364	4.01%
7	1.421	1.312	7.67%	1.291	9.15%	1.324	6.38%
8	0.96	1.21	16.77%	1.042	8.54%	0.912	5.00%
9	1.55	1.364	12.00%	1.391	10.26%	1.614	4.13%
10	0.87	1.007	15.75%	0.973	11.84%	0.964	10.80%

Figure 3 shows the predicted slope steady state of different models, and the GM-RBF model can prevent the slope collapse in time, which tends to be consistent with the actual steady state. In the sample sequence 1-10, the GM(1,5) model has an error of 1 in samples 5 and 6, and the RBF model has the same error of 1 in samples 6-10.The GM-RBF model has an error of 0, and the predicted state is very stable, with high applicability and reliability, and it can be widely applied to help people to avoid potential dangers.

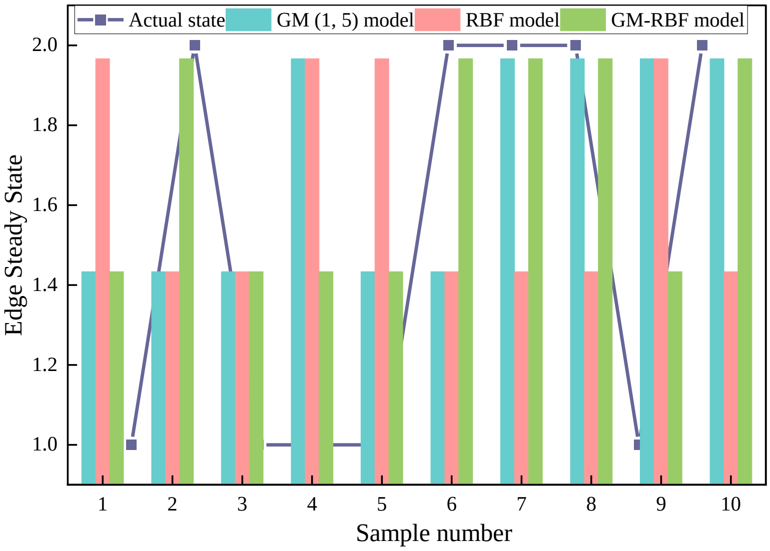

Figure 3 Prediction of slope steady state with different models

6. CONCLUSION

In this paper, we collect the characteristics of terrain and landforms to obtain the characteristic data of terrain and landforms. Based on the collected data, a model for predicting the stability of slopes is established by using gray system theory to complete the prediction of slope stability. In order to comprehensively analyze the performance of the model, the effect of the model in predicting slope stability is analyzed from three perspectives: slope stability prediction, slope displacement and deformation, and slope safety analysis. Among them. Under the conditions of the cohesion force of 22kM and the cohesion force of the slope is 0kPa, the value of the predicted safety coefficient is 1.15, and the value of the actual safety coefficient is 1.13, and the error of the two is less. In addition, it was found that the constructed prediction model GM-RBF has higher accuracy in prediction compared to the other two models. Even when predicting the horizontal displacement, the predicted and actual measured values of the model are 1.2, and the predicted and actual values of the vertical displacement are -0.5. It proves that the stability of slopes can be accurately predicted, and the slopes can be stabilized in time to prevent dangerous situations, which promotes the development of slope engineering.

REFERENCES

[1] Yang, Y., Zhou, W., Jiskani, I. M., Lu, X., Wang, Z., & Luan, B. (2023). Slope stability prediction method based on intelligent optimization and machine learning algorithms. Sustainability, 15(2), 1169.

[2] Marrapu, B. M., Kukunuri, A., & Jakka, R. S. (2021). Improvement in prediction of slope stability & relative importance factors using ANN. Geotechnical and Geological Engineering, 39(8), 5879-5894.

[3] Gu1a, Y. T., Xu2b, Y. X., Moayedi, H., Zhao5c, J. W., & Le, B. N. (2022). Slope stability prediction using ANFIS models optimized with metaheuristic science.

[4] Ray, A., Kumar, V., Kumar, A., Rai, R., Khandelwal, M., & Singh, T. N. (2020). Stability prediction of Himalayan residual soil slope using artificial neural network. Natural Hazards, 103(3), 3523-3540.

[5] Mahmoodzadeh, A., Mohammadi, M., Farid Hama Ali, H., Hashim Ibrahim, H., Nariman Abdulhamid, S., & Nejati, H. R. (2022). Prediction of safety factors for slope stability: comparison of machine learning techniques. Natural Hazards, 1-29.

[6] Huang, S., Huang, M., & Lyu, Y. (2020). An Improved KNN-Based Slope Stability Prediction Model. Advances in Civil Engineering, 2020(1), 8894109.

[7] Markovic Brankovic, J., Andrejevic Stosovic, M., Zivkovic, S., & Brankovic, B. (2021). ANN model for prediction of rockfill dam slope stability. Tehnički vjesnik, 28(5), 1488-1494.

[8] Pei, T., Qiu, T., & Shen, C. (2023). Applying knowledge-guided machine learning to slope stability prediction. Journal of Geotechnical and Geoenvironmental Engineering, 149(10), 04023089.

[9] Meng, J., Mattsson, H., & Laue, J. (2021). Three-dimensional slope stability predictions using artificial neural networks. International Journal for Numerical and Analytical Methods in Geomechanics, 45(13), 1988-2000.

[10] Xie, H., Dong, J., Deng, Y., & Dai, Y. (2022). Prediction model of the slope angle of rocky slope stability based on random forest algorithm. Mathematical Problems in Engineering, 2022(1), 9441411.

[11] Liu, L., Zhao, G., & Liang, W. (2023). Slope stability prediction using K-NN-based optimum-path forest approach. Mathematics, 11(14), 3071.

[12] Zhang, H., Wu, S., Zhang, X., Han, L., & Zhang, Z. (2022). Slope stability prediction method based on the margin distance minimization selective ensemble. Catena, 212, 106055.

[13] Dallas, J., Cole, M. P., Jayakumar, P., & Ersal, T. (2021). Terrain adaptive trajectory planning and tracking on deformable terrains. IEEE Transactions on Vehicular Technology, 70(11), 11255-11268.

[14] Dallas, J., Jain, K., Dong, Z., Sapronov, L., Cole, M. P., Jayakumar, P., & Ersal, T. (2020). Online terrain estimation for autonomous vehicles on deformable terrains. Journal of Terramechanics, 91, 11-22.

[15] Chen, Z., Ma, X., Li, H., Xu, X., & Han, X. (2024). Intelligent terrain generation considering global information and terrain patterns. Computers & Geosciences, 182, 105482.

[16] Zhang, L., Wang, P., Huang, C., Ai, B., & Feng, W. (2021). A method of optimizing terrain rendering using digital terrain analysis. ISPRS International Journal of Geo-Information, 10(10), 666.

[17] Zhang, L., Guo, D., & Wu, J. (2023). Rocky slope stability prediction model and its engineering application based on the VIKOR and binary semantics. KSCE Journal of Civil Engineering, 27(8), 3300-3312.

[18] Qin, J., Ye, J., Sun, X., Yong, R., & Du, S. (2023). A single-valued neutrosophic Gaussian process regression approach for stability prediction of open-pit mine slopes. Applied Intelligence, 53(11), 13206-13223.

[19] Lin, S., Zheng, H., Han, B., Li, Y., Han, C., & Li, W. (2022). Comparative performance of eight ensemble learning approaches for the development of models of slope stability prediction. Acta Geotechnica, 17(4), 1477-1502.

[20] Wang, S., Zhang, Z., & Wang, C. (2023). Prediction of stability coefficient of open-pit mine slope based on artificial intelligence deep learning algorithm. Scientific reports, 13(1), 12017.

[21] Haider, M., Yuan, S., Li, T., Liu, Y., Lawrence, D. D., & Khan, R. K. M. (2023). Stability prediction of the toppling rock slope on the Heihe reservoir bank using discontinuous deformation analysis. Environmental Earth Sciences, 82(16), 383.

FUNDING

This work was supported by 'the Science and Technology Plan Project of Yunnan Province Science and Technology Department' (Grant No.202101BA070001-145).

ABOUT THE AUTHOR

Zhongcai Gao

Faculty of Land Resources Engineering ,Kunming University of Science and Technology, Kunming 650093, Yunnan, China.

E-mail: 2653101881@qq.com

Huiqian Zhang

Faculty of Land Resources Engineering ,Kunming University of Science and Technology, Kunming 650093, Yunnan, China.

E-mail: hannibalnn@163.com

Jiangqin Chao

School of Geographical Sciences and Tourism, Zhaotong University, Zhaotong 657000, Yunnan, China.

E-mail:China.15987138961@163.com

Yurong Li

Faculty of Land Resources Engineering ,Kunming University of Science and Technology, Kunming 650093, Yunnan, China.

E-mail: 1544781823@qq.com

YongjunLi

Faculty of Land Resources Engineering ,Kunming University of Science and Technology, Kunming 650093, Yunnan, China.

E-mail: 1648154044@qq.com

Jiale An

Faculty of Civil Engineering and Mechanics ,Kunming University of Science and Technology, Kunming 650500, Yunnan, China.

E-mail: 1870021348@qq.com